bodies ($m = \frac{3}{4}$) are given. The atmosphere assumed was

$$M_\infty \nu_\infty / u_\infty = E10^{(h-350)/50}$$

where $1 \leq E \leq 2$ for $100 \leq h$ (kft) ≤ 400. The optimum thickness ratio α_m is proportional to $M_\infty^{2/3}/Re_b^{1/3}$ where Re_b is the flight Reynolds number referred to base radius. The validity of the theory is bounded at low altitudes by the assumption that the bow-shock is strong, and at high altitudes by the assumptions of no slip and no shock-layer merging. The results are useful primarily for $0.1 \leq r_b(\text{ft}) \leq 10.0$ at altitudes in the range $200 \leq h(\text{kft}) \leq 300$. Under these conditions the optimum slenderness, for minimum drag, is $\alpha_m = 0.1$ radians (approximately).

Slender Bodies of Minimum Drag in Hypersonic Viscous Flow

HAROLD MIRELS* AND JOHN W. ELLINWOOD†
The Aerospace Corporation, El Segundo, Calif.

Hypersonic viscous flow about slender cones, wedges, and $\frac{3}{4}$ power law bodies is considered. Body thickness ratios leading to minimum drag are determined subject to constraints of fixed base, fixed volume, or fixed surface area. It is assumed that the shocks are strong and that the fluid is ideal. It is found that minimum drag occurs in a flow region where viscous interaction and, for axisymmetric bodies, transverse curvature must be taken into account. For a given body shape and base radius, the optimum thickness ratio α_m is proportional to $M_\infty^{2/3}/Re_b^{1/3}$ where M_∞ is the flight Mach number and Re_b is the flight Reynolds number referenced to base radius. Numerical results are given for optimum thickness ratio and minimum drag as a function of altitude. The results are useful primarily for base radii between 0.1 and 10 ft at altitudes between 2×10^5 and 3×10^5 ft.

Nomenclature

B = $(1 + 3.46\, g_w)M_\infty(CL/Re)^{1/2}$
C = Chapman-Rubesin constant, $\mu_r T_\infty/\mu_\infty T_r$
C_D = drag coefficient referenced to base area
$C_D{}^r$ = Eq. (3)
$C_D{}^V$ = Eq. (5)
$C_D{}^S$ = Eq. (7a)
g_w = T_w/T_0
h = altitude
L = vehicle length
M_∞ = freestream Mach number u_∞/a_∞
m = power law exponent $r_w \sim x^m$
Pr = Prandtl number
Re = Reynolds number $\rho_\infty u_\infty L/\mu_\infty$
Re_b = $\rho_\infty u_\infty r_b/\mu_\infty$
r = transverse distance
$r_w(x), r_b$ = body ordinate; value at base
S = surface area (symmetric body assumed for σ = o case)
T = temperature
T_0 = freestream stagnation temperature
u_∞ = freestream velocity
V = volume (symmetric body assumed for σ = o case)
x = axial distance
α = r_b/L
α_e = $(r_b + \delta_b^*)/L$
$\alpha_m{}^r$ = Eq. (4)
$\alpha_m{}^V$ = Eq. (6)
$\alpha_m{}^S$ = Eq. (7b)
γ = ratio of specific heats
δ_b^* = boundary-layer displacement thickness at base
$\bar{\Lambda}$ = $(1 + 3.46\, g_w)(M_\infty/\alpha^2)(C/Re)^{1/2}$
μ = viscosity
ρ = density
σ = 0, 1 for two-dimensional or axisymmetric bodies, respectively
ψ = C_D/α^2

Subscripts

m = minimum drag value
∞ = freestream value

Received October 22, 1969; revision received February 27, 1970. This work was supported by the U.S. Air Force under contract F04701-69-C-0066.

* Head, Aerodynamics and Heat Transfer Department, Laboratories Operations. Associate Fellow AIAA.

† Member of the Technical Staff, Laboratories Operations. Associate Fellow AIAA.

I. Introduction

THE determination of body shapes with minimum drag subject to certain constraints is of importance in aerodynamic design. A recent survey of activities in this area is given in Ref. 1.

Consider the following problem: given the base radius, volume, or surface area of a plane or axisymmetric body in a hypersonic flow, what forebody shape will yield minimum drag? This problem does not appear to have been treated in the literature with a realistic consideration of boundary-layer effects. For instance, in Ref. 1, viscous interaction and transverse curvature effects are neglected, and a Newtonian pressure distribution and a constant local skin-friction coefficient are assumed. Furthermore, the local skin-friction coefficient is assumed to be known, a priori, and its dependence on the local pressure is ignored. It is shown herein that viscous interaction and (for axisymmetric bodies) transverse curvature effects need to be taken into account. In addition, the effect of the local pressure on the local shear also needs to be considered. Hence, the results of Ref. 1 appear to be unrealistic.

In the present paper, hypersonic flow about slender cones, wedges, and $\frac{3}{4}$ power law bodies is considered. Body thickness ratios leading to minimum drag are determined subject to constraints of fixed base, volume, or surface area. The results are based on the viscous interaction theory of Refs. 2 and 3.

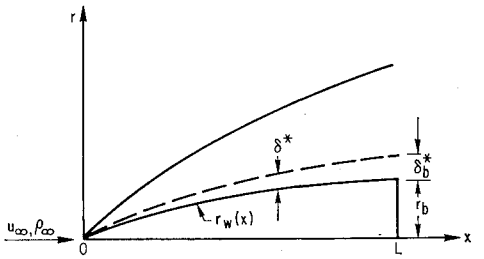

Fig. 1 Slender body in hypersonic flow.

II. Theory

Consider a vehicle flying at constant speed at a constant altitude. A class of power law bodies ($m = \frac{3}{4}, 1$; $\sigma = 0, 1$) that have minimum drag subject to constraints of fixed base height, volume, or surface area will be determined. It is assumed that the flow is hypersonic, $M_\infty^2 \gg 1$; the bodies (including boundary-layer displacement) are slender, $(r_b + \delta_b^*)^2/L^2 \ll 1$; the shocks are strong, $M_\infty^2(r_b + \delta_b^*)^2/L^2 \gg 1$; and the fluid is perfect (Fig. 1).

For a given fluid (γ,Pr), given wall boundary conditions (g_w constant, zero wall blowing, no slip),‡ and a given normalized body shape [$r_w/r_b = f(x/L)$], it has been shown in Refs. 2 and 3

$$C_D/\alpha^2 = \psi(\tilde{\Lambda}) \tag{1a}$$

where

$$\tilde{\Lambda} \equiv BL^{3/2}/r_b^2 \tag{1b}$$

and $B = (1 + 3.46\ g_w)M_\infty(C\nu_\infty/u_\infty)^{1/2}$. The quantity $\tilde{\Lambda}$ is a measure of δ_b^*/r_b and can be termed a "viscous interaction" parameter.[2,3] Values of $\psi(\tilde{\Lambda})$ for $m = \frac{3}{4}, 1$; $\sigma = 0, 1$; $\gamma = \frac{7}{5}$; $g_w = 0$, 0.2, and 0.836 can be deduced from the numerical results in Refs. 2 and 3. The numerical results for $m = \frac{3}{4}$ are exact, while those for $m = 1$ are obtained by an approximate local similarity method. The limiting behavior of

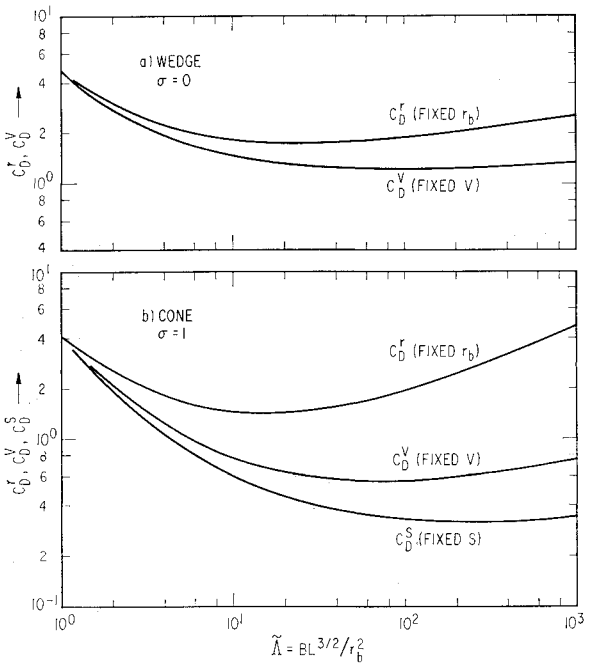

Fig. 2 Variation of drag with $\tilde{\Lambda}$ for fixed r_b, V, or S; $m = 1$, $g_w = 0$, $\gamma = 1.4$, $Pr = 0.7$: a) wedge, b) cone.

‡ Cases with wall blowing and slip can also be treated but are not considered herein.

$\psi(\tilde{\Lambda})$ can be shown to be

$$\psi(\tilde{\Lambda}) = O(1) \qquad \tilde{\Lambda} \to 0 \tag{2a}$$

$$\psi(\tilde{\Lambda}) = O(\tilde{\Lambda}^{(3+\sigma)/2}/\ln^\sigma \tilde{\Lambda}) \qquad \tilde{\Lambda} \to \infty \tag{2b}$$

Equation (2a) corresponds to inviscid flow, while Eq. (2b) corresponds to the strong interaction regime.

Minimum drag bodies with profiles of the form $m = \frac{3}{4}, 1$ and $\sigma = 0, 1$ can now be found under constraints of fixed base, volume, or surface. Each of these constraints is discussed separately.

A. Fixed Base

Consider r_b fixed. Equation (1a) can be written in the form

$$C_D{}^r \equiv C_D r_b^{2/3}/B^{4/3} = \psi/\tilde{\Lambda}^{4/3} \tag{3}$$

For a given flight condition, the left-hand side of Eq. (3) is proportional to vehicle drag, while the right-hand side is a function of only $\tilde{\Lambda}$. It follows from Eqs. (2) that $\psi/\tilde{\Lambda}^{4/3}$ has a minimum at a finite nonzero value of $\tilde{\Lambda}$ (Fig. 2). The value of $\tilde{\Lambda}$ at the point of minimum drag and the corresponding value of $C_D{}^r$ have been obtained for a number of cases using the numerical results of Refs. 2 and 3 and a parabolic fit through three points in the vicinity of the minimum point. The results are given in Table 1. The body slenderness ratio at the minimum drag point

$$\alpha_m{}^r \equiv \alpha_m r_b^{1/3}/B^{2/3} = (\tilde{\Lambda}_m)^{-2/3} \tag{4}$$

is included in Table 1. It is seen that $C_{D,m}{}^{1/2}$ and α_m are proportional to $B^{2/3}/r_b^{1/3} \propto M_\infty^{2/3}/Re_b^{1/3}$.

B. Fixed Volume

Consider a fixed volume $V \equiv Lr_b{}^{\sigma+1}/a$. For a power law body, $a = [(\sigma + 1)m + 1](\sigma + 1)/2\pi^\sigma$. Equation (1a) can be written

$$C_D{}^V \equiv \frac{C_D r_b{}^{(\sigma+1)}\ (aV)^{-(3\sigma+1)/(3\sigma+7)}}{B^{2(3\sigma+5)/(3\sigma+7)}} = \frac{\psi}{\tilde{\Lambda}^{2(3\sigma+5)/(3\sigma+7)}} \tag{5}$$

Again, the left-hand side is proportional to drag, while the right-hand side is a function of $\tilde{\Lambda}$. The drag has a minimum at $\tilde{\Lambda}_m$. Values of $\tilde{\Lambda}_m$ are included in Table 1. The slender-

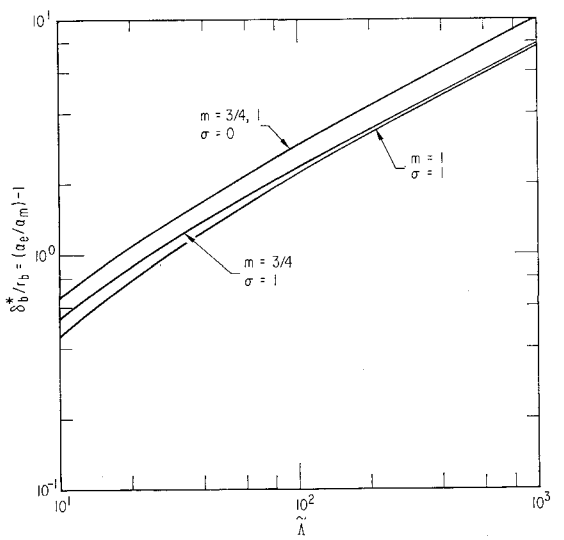

Fig. 3 Boundary layer thickness; $g_w = 0$, $\gamma = 1.4$, $Pr = 0.7$.

Table 1 Parameters at point of minimum drag [$\gamma = 1.4$, $Pr = 0.7$]

			Fixed base radius				Fixed volume				Fixed surface area			
m	σ	g_w	$\tilde{\Lambda}_m$	$\alpha_m{}^r$	$C_{D,m}{}^r$	$\frac{\alpha_e}{\alpha_m}$	$\tilde{\Lambda}_m$	$\alpha_m{}^V$	$C_{D,m}{}^V$	$\frac{\alpha_e}{\alpha_m}$	$\tilde{\Lambda}_m$	$\alpha_m{}^S$	$C_{D,m}{}^S$	$\frac{\alpha_e}{\alpha_m}$
1	0	0.0	23.7	0.121	1.76	2.2	109.	0.0685	1.23	4.1				
		0.2	28.9	0.106	1.18	2.38	127.	0.0628	0.811	4.3				
		0.836	40.5	0.0848	0.703	2.70	193.	0.0495	0.468	5.2				
	1	0.0	15.4	0.162	1.43	1.64	77.7	0.0734	0.577	2.9	303.	0.0382	0.328	5.1
		0.2	16.8	0.152	0.930	1.67	78.0	0.0732	0.372	2.8	283.	0.0397	0.213	4.8
		0.836	22.9	0.124	0.476	1.82	96.2	0.0646	0.178	3.0	383.	0.0334	0.0991	5.3
$\frac{3}{4}$	0	0.0	51.8	0.0720	2.02	2.94	258.	0.0419	1.30	5.86				
		0.2	69.9	0.0589	1.39	3.32	352.	0.0351	0.868	6.75				
		0.836	112.0	0.0430	0.863	4.05	582.	0.0263	0.518	8.53				
	1	0.0	12.6	0.185	1.60	1.64	82.4	0.0709	0.654	3.1				
		0.2	14.4	0.169	1.05	1.68	83.1	0.0705	0.421	3.08				
		0.836	20.8	0.132	0.555	1.87	107.	0.0382	0.205	3.30				

ness ratio of the minimum drag body is

$$\alpha_m{}^V \equiv \alpha_m(aV)^{1/(3\sigma+7)}/B^{2(\sigma+2)/(3\sigma+7)} = (\tilde{\Lambda}_m)^{-2(\sigma+2)/(3\sigma+7)} \tag{6}$$

It is seen that α_m decreases as V increases, but is relatively insensitive to V. Again, $C_{D,m}$ and α_m increase as B increases.

C. Fixed Surface Area

Consider a fixed surface area $S = Lr_b{}^\sigma/b$. For a power law body $b = (\sigma m + 1)/2\pi^\sigma$, Equation (1a) can be expressed as

$$C_D{}^S \equiv \frac{C_D r_b{}^{\sigma+1}\,(bS)^{-(3\sigma+1)/(3\sigma+4)}}{B^{6(\sigma+1)/(3\sigma+4)}} = \frac{\psi}{(\tilde{\Lambda})^{6(\sigma+1)/(3\sigma+4)}} \tag{7a}$$

where the left-hand side is proportional to vehicle drag. From Eq. (2), it is seen that the right-hand side of Eq. (7a) approaches a constant as $\tilde{\Lambda} \to \infty$, when $\sigma = 0$, and the drag does not have a minimum, at a finite nonzero value of $\tilde{\Lambda}$, for two-dimensional flows. Physically, when $\sigma = 0$ and the surface area is fixed, L is also fixed, and the drag reduces to the flat plate drag as $r_b \to 0$. However, a minimum drag does exist for $\sigma = 1$. Values for this case also are included in Table 1. The body thickness ratio at the minimum drag point, for $\sigma = 1$, is

$$\alpha_m{}^S \equiv \alpha_m(bS)^{1/7}/B^{4/7} = (\tilde{\Lambda})^{-4/7} \tag{7b}$$

and is only weakly dependent on S.

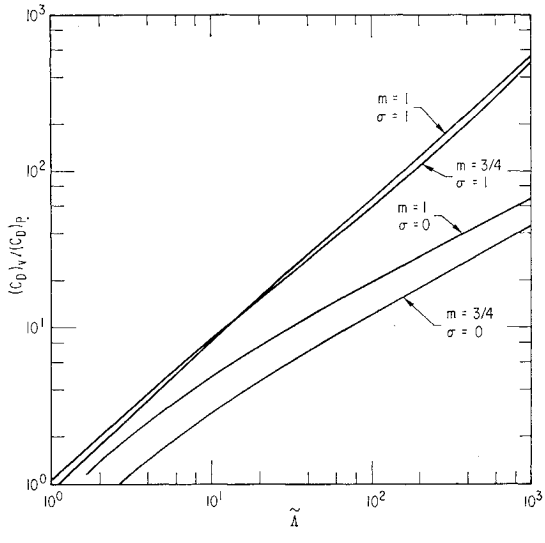

Fig. 4 Ratio of viscous to pressure drag; $g_w = 0$, $\gamma = 1.4$, $Pr = 0.7$.

III. Results and Discussion

The nature of the flow when $\tilde{\Lambda} = \tilde{\Lambda}_m$ and some limitations of the present results are noted below. The quantity $\tilde{\Lambda}$ is a measure of viscous interaction effects and, for $\sigma = 1$, of transverse curvature effects. Table 1 indicates that the minimum drag, for cases treated herein, occurs at values of $\tilde{\Lambda}_m$ in the range $12 < \tilde{\Lambda}_m < 600$. These values of $\tilde{\Lambda}_m$ imply moderate to relatively strong viscous interaction and transverse curvature. Hence, these effects need to be considered when minimum drag bodies are evaluated.

Let $\alpha_e = [(r_b + \delta_b{}^*)/L]_m$ denote the effective body thickness ratio at the minimum drag point. Values of α_e/α_m are in the range $1.5 < \alpha_e/\alpha_m < 8.5$ (Table 1). Hence, the boundary-layer displacement thickness at the base is approximately equal to or greater than the local body thickness. The variation of α_e/α_m with $\tilde{\Lambda}$ is given, for representative cases, in Fig. 3.

The ratio of viscous drag $(C_D)_v$ to pressure drag $(C_D)_p$ is given in Fig. 4. It is seen that $1 \lesssim (C_D)_v/(C_D)_p \lesssim 300$ for

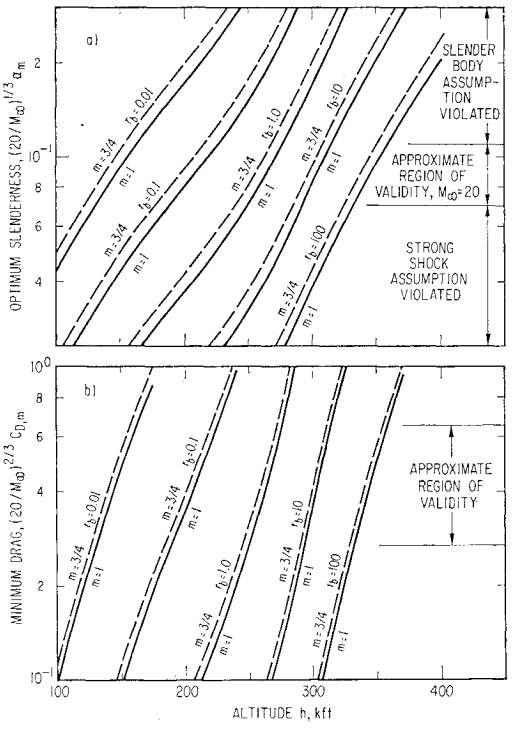

Fig. 5 Effect of altitude on minimum drag body with fixed base r_b, ft; $C = 1$, $g_w = 0$, $\gamma = 1.4$, $Pr = 0.7$: a) optimum slenderness, b) minimum drag coefficient.

Table 2 Quantities defining allowable range of α_m and $l^{(\ )}$ [$Pr = 0.7$, $\gamma = 1.4$, $g_w = 0$, $\sigma = 1$, $M_\infty = 20$, $E = 1.5$]

Constraint	m	Range of α_m, Eq. (8) $\frac{5^{1/2}/20}{\alpha_e/\alpha_m}$, rad	Range of α_m, Eq. (8) $\left(\frac{0.2}{\tilde{\Lambda}_m}\right)^{1/2}$, rad	Range of $l^{(\ )}$, Eq. (9) $\frac{\Lambda_m^2}{EM_\infty}\left(\frac{5^{1/2}\alpha_m}{20\alpha_e}\right)^{(\ )}$, ft^{-1}	Range of $l^{(\ )}$, Eq. (9) $\frac{\tilde{\Lambda}_m^2}{EM_\infty}\left(\frac{0.2}{\tilde{\Lambda}_m}\right)^{(\ )}$, ft^{-1}
r_b	1	0.068	0.11	0.0025	0.012
r_b	$\frac{3}{4}$	0.068	0.13	0.0017	0.011
V	1	0.039	0.051	0.0039	0.013
V	$\frac{3}{4}$	0.036	0.049	0.0035	0.010
S	1	0.022	0.026	0.0048	0.0083

$10 \lesssim \Lambda_m \lesssim 600$. Thus, the viscous drag is equal to or larger than the pressure drag at the point of minimum net drag.

The present theory is based on the assumption that the body is slender, $\alpha_e^2 \ll 1$; that the shock is strong, $\alpha_e^2 M_\infty^2 \gg 1$; and that rarefaction effects are negligible. In Ref. 4 it is suggested that rarefaction effects are negligible in the shock layer§ when $M_\infty/(Re)^{1/2} \equiv \alpha_m^2\tilde{\Lambda}_m \ll 1$. These conditions are approximately satisfied when $\alpha_e^2 \lesssim 0.2$, $\alpha_e^2 M_\infty^2 \gtrsim 5$, and $\alpha_m^2\tilde{\Lambda}_m \lesssim 0.2$, respectively. In the present cases, $\alpha_e^2 \lesssim 0.2$ is always satisfied when $\alpha_m^2\tilde{\Lambda}_m \lesssim 0.2$. Hence, the range of values of α_m, for which the present theory is valid, is

$$(5^{1/2}/M_\infty)(\alpha_m/\alpha_e) \lesssim \alpha_m \lesssim (0.2/\tilde{\Lambda}_m)^{1/2} \tag{8}$$

The range is quite small (Table 2).

The effect of altitude on allowable body scale can be readily determined. Note that $B = M_\infty^{1/2}(M_\infty L/Re)^{1/2}$ when $C = 1$ and that for a standard atmosphere $M_\infty L/Re = E10^{(h-350/)50}$ where $1 \leq E \leq 2$ for $100 \leq h$, kft ≤ 400.

Using this atmospheric model and Eqs. (4, 6, and 7b), one finds that, for each of the three constraints, the altitude range and allowable body scale length l are related through one of the following inequalities:

$$(\tilde{\Lambda}_m^2/EM_\infty)[(5^{1/2}/M_\infty)\alpha_m/\alpha_e]^3 \lesssim 10^{h/50-7}/l^r \lesssim (\tilde{\Lambda}_m^2/EM_\infty)(0.2/\tilde{\Lambda}_m)^{3/2} \tag{9a}$$

$$\frac{\Lambda_m^2}{EM_\infty}\left(\frac{5^{1/2}}{M_\infty}\frac{\alpha_m}{\alpha_e}\right)^{(3\sigma+7)/(\sigma+2)} \lesssim \frac{10^{h/50-7}}{l^V} \lesssim \frac{\tilde{\Lambda}_m^2}{EM_\infty}\left(\frac{0.2}{\tilde{\Lambda}_m}\right)^{(3\sigma+7)/(2\sigma+2)} \tag{9b}$$

$$(\tilde{\Lambda}_m^2/EM_\infty)[(5^{1/2}/M_\infty)\alpha_m/\alpha_e]^{7/2} \lesssim 10^{h/50-7}/l^S \lesssim (\tilde{\Lambda}_m^2/EM_\infty)(0.2/\tilde{\Lambda}_m)^{7/4} \tag{9c}$$

where $l^r \equiv r_b$, $l^S \equiv (Lr_b{}^{\sigma+1})^{1/(\sigma+2)}$ and $l^S \equiv (Lr_b)^{1/2}$, the last pertaining to axisymmetric bodies only. Equations (9) have been evaluated for $M = 20$, and the results are included in Table 2. It is seen that the present theory is useful, primarily, for altitudes in the range $200 \lesssim h$, kft $\lesssim 300$, for bodies in the range $0.1 \lesssim r_b$, ft $\lesssim 10$.

Optimum slenderness α_m and the corresponding minimum drag coefficient $C_{D,m}$ are given in Figs. 5–7 as a function of altitude for various geometric scales. For a given geometric scale, both $C_{D,m}$ and α_m increase with altitude since B increases with altitude.

IV. Concluding Remarks

It has been shown that slender bodies in hypersonic flow have a minimum drag at a fixed value of $\tilde{\Lambda}_m \sim B/r_b\alpha_m^{3/2}$ where $B \sim M_\infty(CL/Re)^{1/2}$. The specific value of $\tilde{\Lambda}_m$ depends

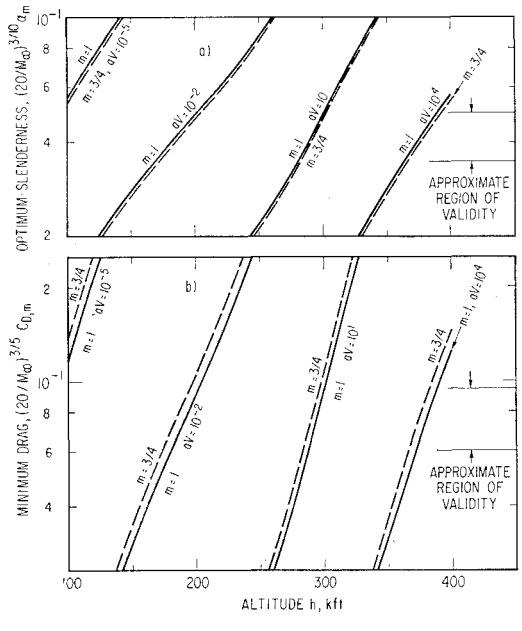

Fig. 6 Effect of altitude on minimum drag body with fixed volume V, ft^3; $C = 1$, $g_w = 0$, $\gamma = 1.4$, $Pr = 0.7$: a) optimum slenderness, b) minimum drag coefficient.

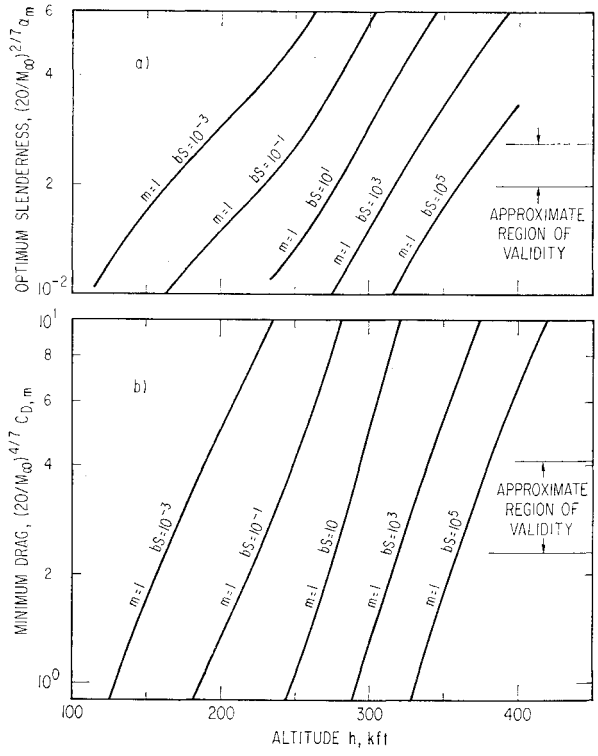

Fig. 7 Effect of altitude on minimum drag body with fixed surface area S, ft^2; $C = 1$, $g_w = 0$, $\gamma = 1.4$, $Pr = 0.7$: a) optimum slenderness, b) minimum drag coefficient.

§ Wall slip effects are negligible when $0.1\ \alpha_m g_w^{1/2}\tilde{\Lambda}_m \ll 1$.[2,3] The quantity $M_\infty/(Re)^{1/2}$ can be used as a measure of the rarefaction effects when $0.1\ g_w^{1/2}/\alpha_m \lesssim 1$.

on the normalized body profile (e.g., m); fluid properties γ, Pr; wall boundary conditions g_w; and geometric constraints. In the cases treated herein, the minimum drag occurred in a region where viscous interaction and transverse curvature effects need to be taken into account.

Consider hypersonic flight at low altitudes, e.g., $h \lesssim 100$ kft. In these cases, B is generally small, and therefore α_m and $C_{D,m}$ are small. Values of α_m are generally too small for practical construction. (In addition, the present strong shock assumption is violated.) With increase in altitude, B, α_m, and $C_{D,m}$ increase. At altitudes of the order 200–300 kft, optimum values of α_m are of the order of 0.1 rad, which are physically practical, and the flow is consistent with the present assumptions.

It would be of interest to relax the present assumptions of a slender body and a strong shock and to treat more general body shapes than $m = \frac{3}{4}, 1$. However, such extensions are beyond the scope of the present paper.

In Ref. 5, slender power law bodies of the form $r_w/r_b = (x/L)^m$ with fixed values of r_b, L have been considered, and the value of m, which minimizes the drag, has been determined as a function of λ. Newtonian slender body theory was assumed, viz., $M_\infty^2 \gg 1$, $(\gamma - 1) \ll 1$, $\alpha^2 \ll 1$, and $(\alpha M_\infty)^2 \gg 1$. Viscous interaction and transverse curvature effects were assumed negligible, i.e., $\delta_b^*/r_b \sim (\gamma - 1)\tilde{\Lambda} \ll 1$. Hence, one can use this reference to find the power law body of minimum drag for fixed r_b, L, and B, provided δ_b^*/r_b is small. However, because viscous interaction is neglected, $C_D \to 0$ as $r_b/L \to 0$. Thus, one can not use Ref. 5 to deduce minimum drag for fixed r_b, B.

Blunt nosed bodies (hemispheres, flat faces) have C_D values in the range $1 \lesssim C_D \lesssim 2$, the value depending on M_∞ and Reynolds number. These C_D values provide a guide for the drag benefit to be derived by use of the optimum slender bodies described herein. Figure 2 can be used to estimate the drag penalty imposed by not using the optimum α.

References

[1] Miele, A., *Theory of Optimum Aerodynamic Shapes*, Academic Press, New York, 1965.

[2] Mirels, H. and Ellinwood, J. W., "Viscous Interaction Theory for Slender Axisymmetric Bodies in Hypersonic Flow," *AIAA Journal*, Vol. 6, No. 11, Nov. 1968, pp. 2061–2070.

[3] Mirels, H. and Ellinwood, J. W., "Hypersonic Viscous Interaction Theory for Slender Axisymmetric Bodies," TR-0158-(3240-10)-1, 1967, The Aerospace Corp., El Segundo, Calif.

[4] McCrosky, W. J., Bogdonoff, S. M., and Genchi, A. R., "Leading Edge Flow Studies in Rarefied Hypersonic Flow," *Proceedings of The 5th International Symposium on Rarefied Gas Dynamics*, Vol. II, Academic Press, New York, 1967, pp. 1047–1066.

[5] Lewellen, W. S. and Mirels, H., "Optimum Lifting Bodies in Hypersonic Viscous Flow," *AIAA Journal*, Vol. 4, No. 10, Oct. 1966, pp. 1866–1868.